

Assimilation and Forecasting Experiments Using Radar Observations and WRF 4DVar

Juanzhen Sun¹, Yongrun Guo¹, Eunha Lim¹, Xiangyu Huang¹, Qingnong Xiao¹, and Soichiro Sugimoto²

(1) National Center for Atmospheric Research, USA

(2) Central Research Institute of Electrical Power Industry, Japan

1. Introduction

In the last decade, the four-dimensional variational (4DVar) technique has been applied to the convective scale to assimilate high-resolution observations such as those from Doppler radars. Sun and Crook (1997; 1998) demonstrated that a 4DVar system, referred to as VDRAS (Variational Doppler Radar Analysis System), based on a cloud-scale numerical model and radar observations (radial velocity and reflectivity) was able to retrieve the model variables (three-dimensional wind, thermodynamics, and microphysics) that are not observed by radars. Later it was shown that the retrieved fields improved very-short-term forecasts of severe storms when used as initial conditions of the cloud-scale model (Sun 2005a; Sun and Zhang 2008). Although these results are encouraging, VDRAS has limited operational applications because the cloud model does not have topography and has only simple physics.

Kawabata et al. (2007) demonstrated that the assimilation of radar radial velocity and GPS precipitable water vapor improved precipitation forecasts of a heavy rainfall event that occurred in Tokyo using a nonhydrostatic model that has operational capability. In this study, we expand our previous radar data assimilation studies by using the more realistic cloud-resolving model WRF (Weather Research and Forecasting) and its 4DVar (Huang et al. 2008). A case study is presented in this paper to show the capability of WRF 4DVAR in radar data assimilation and impact on forecast a convective system that was observed during the IHOP (International H₂O) experiment.

2. WRF 4DVar

WRF 4DVar was developed as an extension of WRF 3DVar (Barker et al. 2004). It has the incremental formulation (Courtier et al. 1997). A detailed description can be found in Huang et al. 2008. It makes use of many pre-existing components of WRF 3DVar, including observation operator, quality control, background error covariance, minimization inner-loop assuming Gaussian error covariances, and iterative outer loop to account for the effect of nonlinearities in the assimilation algorithm. In the outer loop, the full WRF nonlinear model is run to update the basic state from which the tangent linear model is derived. The tangent linear and the adjoint models are executed in the inner loop for the minimization. At present, the tangent linear and adjoint model include the full dynamics, a simple vertical diffusion scheme with surface friction, and a large-scale condensation scheme. More work is underway to add more physics to the inner loop.

The cost function is the summation of the three terms: the background term, the observation term, and the balancing constraint term. A number of variable transformations are operated to the model prognostic variables to precondition the cost function and to enforce balance constraints.

Consequently, the control variables of the cost function are stream function, unbalanced velocity potential, unbalanced temperature, pseudo relative humidity, and unbalanced surface pressure. The final analysis increment includes the x- and y-components of velocity, temperature, water vapor, and surface pressure.

For radar data assimilation, a number of modifications were made (Xiao et al. 2005, 2007). First, vertical velocity increment is added to the analysis variables via the Richardson balance equation, which combines the continuity equation, adiabatic thermodynamic equation, and hydrostatic relation. Second, the total water is used as the moisture control variable, instead of the pseudo relative humidity, for the assimilation of radar reflectivity. The partitioning of the total water into water vapor, cloud water, and rainwater is then achieved by using a warm-rain parameterization scheme. Lastly, the observation operators for assimilating Doppler radar radial velocity and reflectivity are developed.

3. Overview of the IHOP 12-13 June 2002 case

Several convective systems occurred during June 12 and 13 2002 in the IHOP domain. This study focuses on the squall line initiated east of a triple point (intersection of a outflow and a dryline; marked by "T" in Fig. 1a) near the Oklahoma-Kansas border around 2100 UTC and propagated southeastward. Fig. 1 shows the convective activity at two different times by the merged reflectivity field at 0.5° elevation angle from multiple WSR-88D radars and NCAR's S-Pol (S-band dual-polarization Doppler radar). The merging of the radar reflectivity was done by choosing the maximum reflectivity at each grid point from data values given by different radars. A composite map of surface wind observations (white barbs) from several surface networks are overlaid. The blue wind barbs are surface observations from the METAR (METEorological Aerodrome Reports) stations. The radar locations are marked by the radars' names in red letters. Several mesoscale boundaries, including a nearly stationary outflow boundary from previous day convection (orange broken line in Fig. 1a), a dry line (pink line), and a weak cold front (brown line), are observed. A mesoscale circulation (mesoscale low) around the triple point is evidently shown by the surface observations. The warm, moist air mass to the east of the dryline and south of the outflow boundary contained CAPE near 2000 J kg⁻¹ and little CIN (convective inhibition) around 2100 UTC. The air mass to the north of the outflow boundary is slightly cooler.

Convective cells are developing east of the triple point and are clearly visible at 2120 UTC (Fig. 1a). The thunderstorm near the triple point intensified and new storms were developed near the Oklahoma-Kansas border as the circulation associated with the mesoscale low strengthened. Damaging winds and large hail were reported

in conjunction with some of the storms. The severe storm near the triple point produced golf-ball-size hail, maximum outflow wind speeds exceeding 30 m/s, flashing flood, and at least one tornado. By 0200 UTC, a well-organized squall line had developed (Fig. 1b) and it then moved southeastward. The squall line is reduced in spatial extension at 0400 UTC and completely dissipated around 0900 UTC. The stage-IV precipitation analysis of the National Centers for Environmental Prediction reported a maximum 3-hr rainfall accumulation of 89.5 mm at 0300UTC in north Oklahoma. Our focus in the current study is not on the prediction of the initial storm development, but the prediction of evolution of existing storms and development of new ones from outflow interaction.

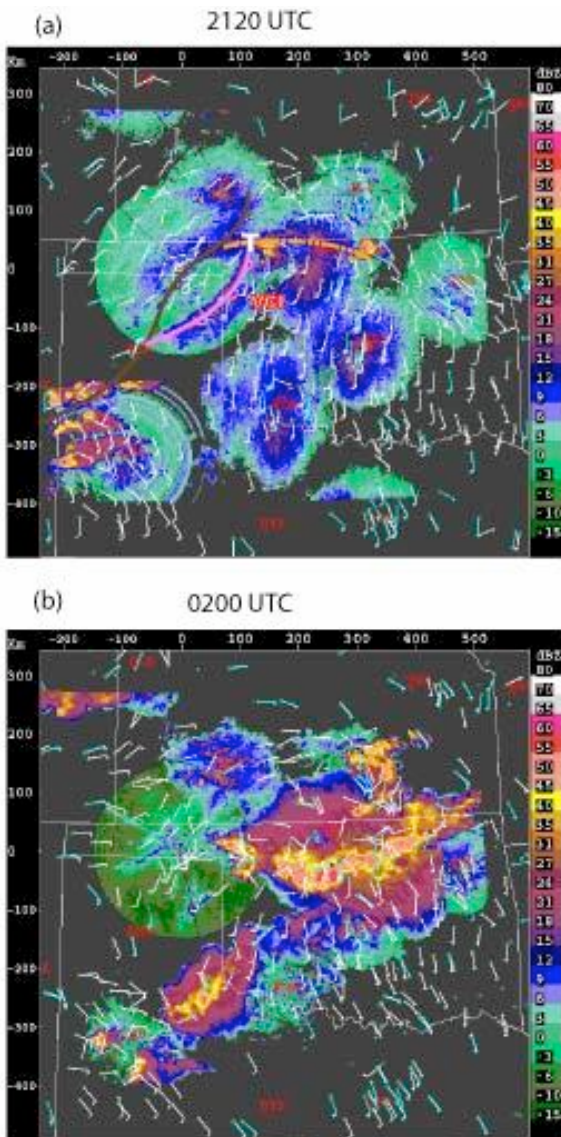


Fig. 1 Merged radar reflectivity image using the 0.5° elevation angle data at 2120 UTC (a) and 0200 UTC. The surface wind from METAR is shown by cyan wind barb and from a composite of all surface networks is shown by white. The cold front (brown line), dryline (pink line), and outflow boundary (dashed orange) are depicted in (a).

The radar data preprocessing quality control follows closely the procedure in VDRAS (Sun 2005b). It includes interpolating data from radar spherical coordinates to

uniformly gridded data on elevation angle surfaces, noise removal, velocity unfolding, void filling, and superobbing, and estimation of observation errors.

4. OSSE experiments and results

We first conducted OSSE (Observing System Simulation Experiment) by composing radial velocity and reflectivity data from a control simulation. This control simulation was initiated at 1200 UTC on 12 June using AWIP 40 km analysis and run for 24 hours. The simulation was run on a nested domain with 12km and 4km resolution. The physics options include the Thompson microphysics (Thompson et al. 2004), Noah land surface model, and Yonsei University boundary layer scheme. The 4DVar radar data assimilation was conducted with a time window of 15 min. starting at 0100 UTC on 13 June. The data assimilation domain covers an area of 604km x 472km with a resolution of 4km (Fig. 2). There are 10 radars in or near the 4DVar domain, each located at the actual site of the NEXRAD network. The radar velocity and reflectivity data were computed using data from the control simulation based on the following relationships, respectively:

$$V_r = \frac{1}{R}[(x_d - x_r)u + (y_d - y_r)v + (z_d - z_r)(w - V_t)] \quad (1)$$

$$Z = 43.1 + 17.5 \log(\rho q_r) \quad (2)$$

These data were assumed to have a temporal interval of 5 min. We ALSO assume that both the radial velocity and reflectivity are available only at the grid points where the reflectivity is greater than 5 dBZ and there are no data above the 20° elevation angle and beyond 200km from each radar. Fig. 3a shows the

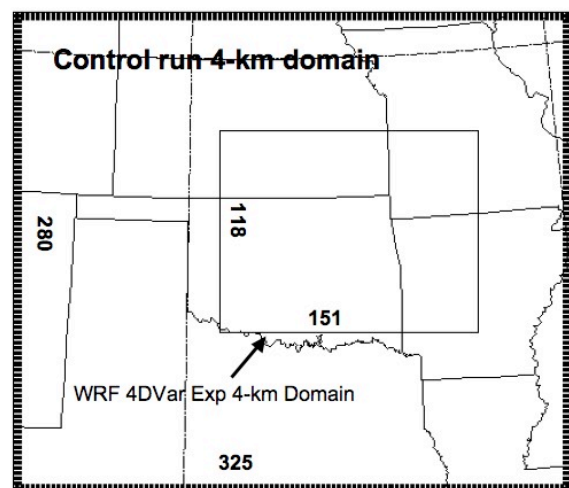


Fig. 2 The 4km domain of the control simulation and the 4DVar data assimilation domain. The numbers show the grid points on each domain.

radar location and the 200km ring for each radar. Fig. 3b shows the data coverage area at 0100 UTC.

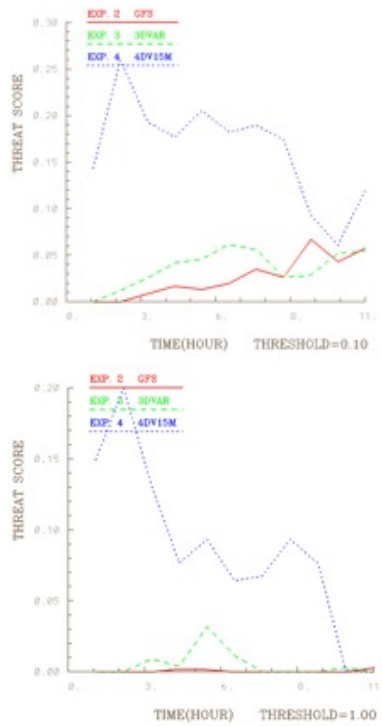


Fig. 5 Threat score of hourly precipitation with respect to forecast hour for thresholds of 0.1 cm and 1.0 cm from the OSSEs.

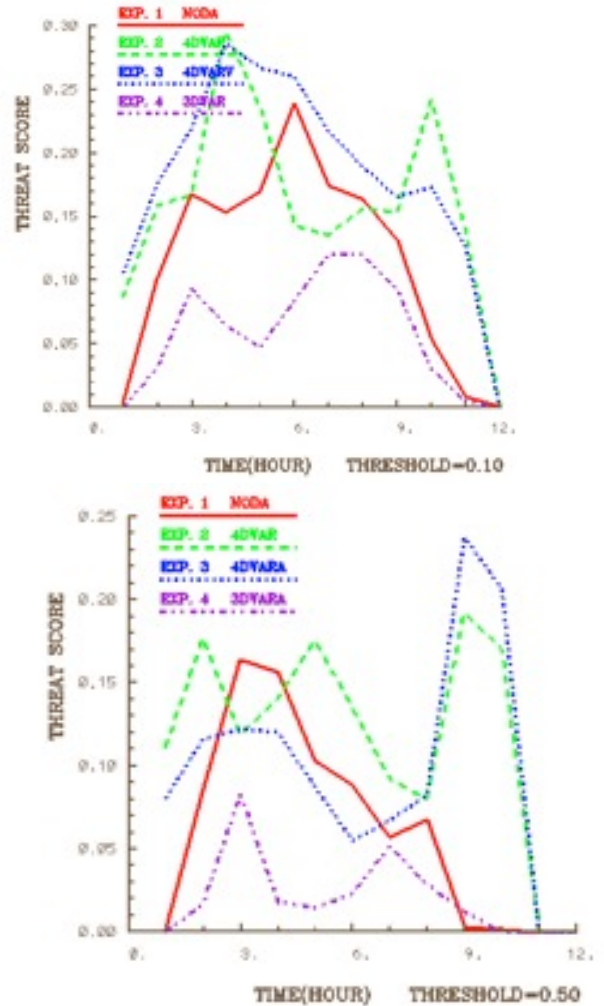


Fig. 7 Threat score of hourly precipitation with respect to forecast hour for thresholds of 0.1 cm and 0.5 cm from the real data experiments.

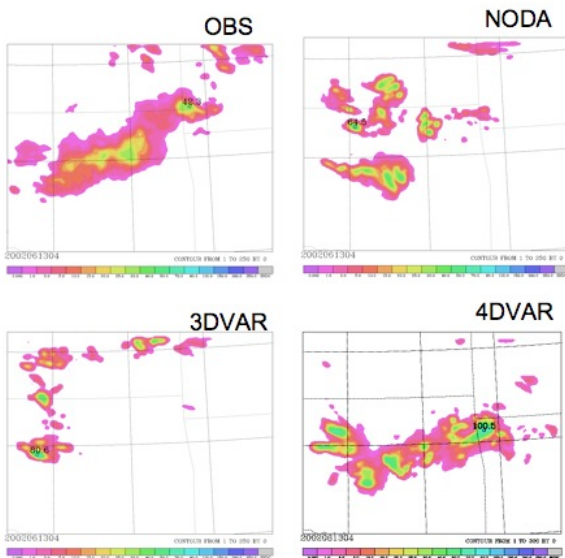


Fig. 6 Fig. 4 4h forecasts, starting at 0000 UTC, 12 June, of hourly-accumulated precipitation from NODA, 3DVAR, and 4DVAR of the real data experiments.

The quality of the precipitation forecasts is also evaluated by computing the threat score. Fig. 7 shows the result. Both 4DVAR and 4DVARA improve the threat score at most of the forecast times over NODA and 3DVARA.

6. Summary and conclusions

OSSE and real data experiments are performed to examine the feasibility and impact of assimilating Doppler radar radial velocity on forecasting of severe convective weather. A case of squall line that occurred during the IHOP experiment is used for the study. Both the OSSE and the real data experiments show that the assimilation of radial velocity using WRF 4DVAR improves the short-term precipitation forecasts over WRF 3DVAR and the experiments that do not have radar data assimilation. Work is still in progress to examine the sensitivity of the 4DVAR analysis and forecast with respect to assimilation window and domain size.

7. Acknowledgement

This study is sponsored the Central Research Institute of Electrical Power Industry of Japan. The authors wish to thank Xin Zhang and Yunsheng Chen for software engineering support on this work.

8. References

- Barker, D. M., W. Huang, Y. R. Guo, and Q.N. Xiao., 2004: A Three-Dimensional (3DVAR) Data Assimilation System For Use With MM5: Implementation and Initial Results. *Mon. Wea. Rev.*, **132**, 897-914.
- Courtier, P., 1997: Dual formulation of four dimensional variational assimilation. *Quart. J. Roy. Meteor. Soc.*, **123**, 2449-2461.
- Crook, N., A., and J. Sun, 2002: Assimilating radar, surface and profiler data for the Sydney 2000 forecast demonstration project. *J. Atmos. Oceanic Technol.*, **19**, 888-898.
- Kawabata T., H. Seko, K. Saito, 2007: An assimilation and forecasting experiment of the Nerima heavy rainfall with a cloud-resolving nonhydrostatic 4-dimensional variational data assimilation system. *J. Meteor. Soc. Japan*, **85**, 255-276.
- Huang X., Q. Xiao, D. M. Barker, X. Zhang, J. Michalakes, W. Huang, T. Henderson, J. Bray, Y. Chen, Z. Ma, J. Dudhia, Y. Guo, X. Zhang, D-J Won, H-C Lin, Y-H Kuo, 2008: Four-dimensional variational data assimilation for WRF: formulation and preliminary results. Submitted to *Mon. Wea. Rev.*
- Sun, J., and N. A. Crook, 1997: Dynamical and microphysical retrieval from Doppler radar observations using a cloud model and its adjoint: Part I. model development and simulated data experiments. *J. Atmos. Sci.*, **54**, 1642-1661.
- Sun, J., and N.A. Crook, 1998: Dynamical and microphysical retrieval from Doppler radar observations using a cloud model and its adjoint: Part II. Retrieval experiments of an observed Florida convective storm, *J. Atmos. Sci.*, **55**, 835-852.
- Sun, J., and N. A. Crook, 2001: Real-time low-level wind and temperature analysis using single WSR-88D data, *Wea. Forecasting*, **16**, 117-132.
- Sun, J., 2005a: Initialization and numerical forecasting of a supercell storm observed during STEPS. *Mon. Wea. Rev.*, **133**, 793-813.
- Sun, J., 2005b: Convective-scale assimilation of radar data: progress and challenges. *Q. J. R. Meteorol. Soc.*, **131**, 3439-3463.
- Sun, J., and Y. Zhang, 2007: Assimilation of multiple WSR_88D Radar observations and prediction of a squall line observed during IHOP. *Mon. Wea. Rev.*, in press.
- Thompson, G., R. M. Rasmussen, and K. Manning, 2004: Explicit forecasts of winter precipitation using an improved bulk microphysics scheme. Part I: Description and sensitivity analysis. *Mon. Wea. Rev.*, **132**, 519-542.
- Xiao, Q., Y.-H. Kuo, J. Sun, W.-C. Lee, E. Lim, Y. Guo, D. M. Barker, 2005: Assimilation of Doppler radar observations with a regional 3D-Var system: impact of Doppler velocities on forecasts of a heavy rainfall case. *J. Appl. Meteor.* **44**, 768-788.
- Xiao, Q., Y.-H. Kuo, J. Sun, W.-C. Lee, and D. Barker, 2007: An Approach of Doppler Reflectivity Data Assimilation and its Assessment with the Inland QPF of Typhoon Rusa (2002) at Landfall, *J. Appl. Meteor.*, **46**, 14-22.
- Xiao, Q., and J. Sun, 2007: Multiple Radar Data Assimilation and Short-range QPF of a Squall Line observed during IHOP_2002. *Mon. Wea. Rev.*, **135**, 3381-3404.